

Dedicated to the memory of Prof. dr. Ioan Silaghi-Dumitrescu marking 60 years from his birth

KINETIC STUDIES OF SORPTION OF COPPER(II) IONS ONTO DIFFERENT CALCIUM-HYDROXYAPATITE MATERIALS

ERZSÉBET-SÁRA BOGYA*, IOAN BÂLDEA, RÉKA BARABÁS,
ALEXANDRA CSAVDÁRI, GRAZIELLA TURDEAN,
VALENTINA-ROXANA DEJEU

ABSTRACT. A study on the removal of copper ions from aqueous solutions by synthetic hydroxyapatite and structurally modified apatite has been carried on under batch conditions. The influence of different sorption parameters, such as heat treatment of the material, particle size, initial metal ion concentration and temperature has been studied and discussed. Maximum adsorption capacity and efficiency were determined. The results showed that the removal efficiency of Cu(II) by hydroxyapatite containing silica (HAP-Si) could reach 99.7%, when the initial Cu(II) concentration was 5 mM. The mechanism of the sorption process was studied, by employing pseudo-first, pseudo-second-order kinetic models and intraparticle diffusion model. Activation energy for hydroxyapatite and 10%_{wf} silica doped hydroxyapatite was obtained, considering pseudo-second-order kinetics model.

Keywords: *hydroxyapatite, modified hydroxyapatite, copper removal, kinetics, diffusion, activation energy*

INTRODUCTION

Hydroxyapatite (HAP) is a mineral, from the group of apatites, having the chemical formula $\text{Ca}_{10}(\text{PO}_4)_6(\text{OH})_2$. Among the different calcium phosphates, hydroxyapatite is the most important bioceramic used in dentistry and orthopedic surgery [1-3]. One way to enhance the bioactive behavior of hydroxyapatite is to obtain substituted apatite, which resemble the chemical composition and structure of the mineral phase in bones. These ionic substitutions can affect the surface structure and charge of hydroxyapatite, which could have an influence on the material in biological environment. In this sense, an interesting way to improve the bioactivity of hydroxyapatite is the addition of silicon to the apatite structure, taking into account the influence

* Babeș-Bolyai University, Faculty of Chemistry and Chemical Engineering, 11 Arany János Str., RO-400084 Cluj-Napoca, Romania, bogyaes@ubbcluj.ro

of this element on the bioactivity of bioactive glasses and glass-ceramics [4,5]. In addition, several studies have revealed the considerable importance of silicon on bone formation and growth under *in vitro* and *in vivo* conditions [6].

Apatite can be used for remediation of soil and water from industrial and nuclear wastes due to their ability to retain a variety of ionic species, especially actinides and heavy metals [7,8]. The mechanisms of the metal cations retention are different and include: ion exchange, adsorption, dissolution/precipitation, and formation of surface complexes [9].

The sorption of pollutants from aqueous solution plays an important role in wastewater treatment because it avoids the process of sludge elimination. Well-designed sorption processes have good efficiency and high quality of effluent after treatment. Sorption material can also be recycled. It is therefore understandable that the study of sorption kinetics in wastewater treatment is interesting as it provides insights into the reaction pathways and into the mechanism of sorption reactions. In addition, the kinetics allows the evaluation of the solute uptake rate which in turn controls the residence time of sorbate uptake at the solid–solution interface. Therefore, it is important to predict the rate at which pollutant is removed from aqueous solutions in order to design appropriate sorption treatment plants. To control the sorption kinetics, knowledge of the rate law describing the sorption system is required. The rate law is determined experimentally.

This paper aims to study the sorption of copper(II) ions onto structurally modified apatite, comparing it to normal hydroxyapatite, and establishing the best kinetic model and mechanism.

RESULTS AND DISCUSSION

As described by Sposito (1986) [10], sorption is the loss of a chemical species from an aqueous solution to a contiguous solid phase. Two of the principle mechanisms of sorption include adsorption, the two-dimensional accumulation of matter at the mineral-water interface; and precipitation, the three-dimensional growth of a solid phase. The study of the nature of copper sorption onto apatites represents the aim of this paper.

As mentioned in the experimental section, copper(II) sorption measurements were carried out with five types of material of two different particle sizes ($> 90 \mu\text{m}$ and $< 45 \mu\text{m}$) and with calcined and non-calcined samples for each material at four different copper concentrations (10^{-4} M, 5×10^{-4} M, 10^{-3} M, 5×10^{-3} M).

For all non-calcined materials at the 10^{-3} M copper concentration, the sorption capacity was almost identical, meaning that the η (efficiency) was around 99.7 %, the difference between them consisting in the saturation time. For the calcined samples, the efficiency was about 60-70 % [11, 12].

The sorption efficiency is defined as $\eta = (c_0 - c_i) / c_0$; c_0 being the initial copper concentration, c_i the actual copper concentration at a specific time, and the sorption capacity given as $q_t = c_{ads} / m$; c_{ads} being the adsorbed amount of copper at a specific time in moles, and m the quantity of the material on which it was adsorbed in grams. The effect of the initial concentration of copper ions was also studied. Its efficiency was calculated for each material at four copper nitrate concentrations as presented in the legend of figure 1 ($c_1 = 5$ mM, $c_2 = 1$ mM, $c_3 = 0.5$ mM and $c_4 = 0.1$ mM).

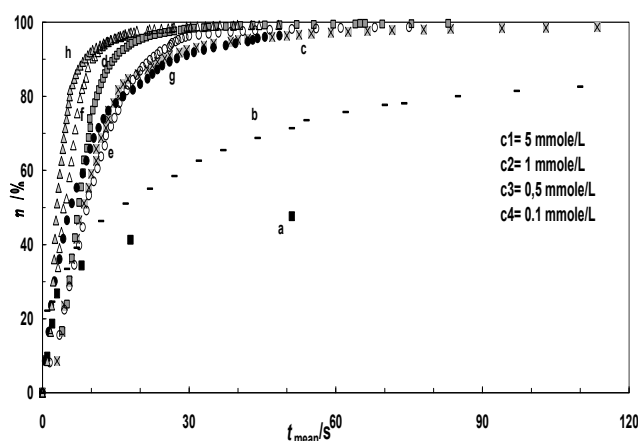


Figure 1. Sorption efficiency for different concentrations and materials as a function of time. of: nCHAP < 45 μ m, c_1 (a); nCHAP-Si 10%_{wt} Si < 45 μ m, c_1 (b); nCHAP < 45 μ m, c_2 (c); nCHAP-Si 10%_{wt} Si < 45 μ m, c_2 (d); nCHAP < 45 μ m, c_3 (e); nCHAP-Si 10%_{wt} Si < 45 μ m, c_3 (f); nCHAP < 45 μ m, c_4 (g); nCHAP-Si 10%_{wt} Si < 45 μ m, c_4 (h).

At the concentration of 5 mM the copper ions sorption efficiency for nCHAP was about 60%, comparable to HAP-Si with 10%_{wt} silica that reaches the efficiency of above 99.6 %, and has the sorption capacity of 20.54 mg/g. CHAP does not sorbs copper ions at such high concentrations and HAP-Si 10%_{wt} Si retains the amount of 50 %. At concentrations lower than 5 mM, sorption takes place at the 99.8 % efficiency for non-calcined materials, and also for calcined materials at concentrations equal or lower than 0.1 mM.

These results show that, for a rapid and complete sorption, the most suitable material is non-calcined silica hydroxyapatite with 10%_{wt} of silica [11, 12].

The increase of temperature enhances the copper sorption for all the studied materials. At higher temperature the end time of the sorption for nCHAP-Si 10%_{wt} silica >45 μ m and 10^{-3} mol/L copper(II) concentration decreases below one minute.

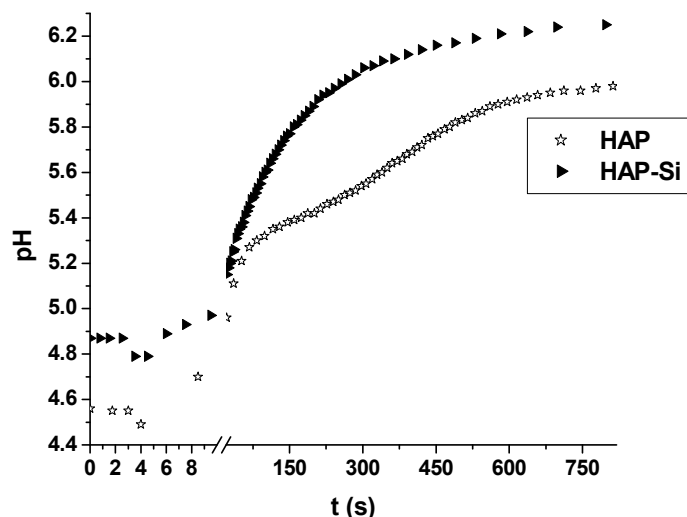


Figure 2. pH variation during the reaction of ncHAP and ncHAP-Si 10%_{wt} $\Phi > 90 \mu\text{m}$ with copper ions ($[\text{Cu}^{2+}] = 10^{-3} \text{ mol/L}$)

Table 1. Initial and final pH in the case of copper nitrate reaction with apatites at 10^{-3} mol/L copper (II) concentration and $T = 293 \text{ K}$

Material	pH _i	pH _f
ncHAP $>90 \mu\text{m}$	5.16	5.75
ncHAP $<45 \mu\text{m}$	5.25	6.08
ncHAP-Si 5% _{wt} Si $>90 \mu\text{m}$	5.2	6.08
ncHAP-Si 5% _{wt} Si $<45 \mu\text{m}$	5.08	6.11
ncHAP-Si 5% _{wt} Si $>90 \mu\text{m}$	5.12	6.46
ncHAP-Si 5% _{wt} Si $<45 \mu\text{m}$	5.11	6.41
ncHAP-Si 10% _{wt} Si $>90 \mu\text{m}$	5.19	6.75
ncHAP-Si 10% _{wt} Si $<45 \mu\text{m}$	5.31	6.52
ncHAP-Si 15% _{wt} Si $>90 \mu\text{m}$	5.11	5.91
ncHAP-Si 15% _{wt} Si $<45 \mu\text{m}$	5.1	5.89

The pH of solution modifies between 4.7 and 6.2 (see figure 2), for $10^{-3} \text{ M Cu}^{2+}$ concentration. Within the initial period of the process, it can be noticed a slight decrease of the pH in the case of materials with higher granulometry. This phenomenon can be caused by ionic exchange between the copper and protons on the superficial $-\text{OH}$ sites. Later increase of pH values is due to the dissolution of the material in the acidic media and base hydrolysis. Table 1 compares the initial and final pH values for all the materials. The highest variation was observed at ncHAP-Si 10%_{wt} Si.

The release of calcium ions during copper(II) sorption was registered with a calcium selective electrode. It was observed that within a very short period calcium concentration increases due to the dissolution of the hydroxyapatite and then decreased significantly. After this initial stage, the calcium release is much slower than the copper sorption and therefore hydrogen ions should be released to maintain the balance of charge. This leads to the conclusion that copper-calcium ion exchange does not control the Cu^{2+} sorption.

Kinetic studies

In order to determine the rate constants, the two mostly used kinetic models in sorption processes, namely pseudo-first and pseudo-second order model, have been checked with our experimental data. Generally, the reaction rate is defined as the change of reactants or products per unit of time. In the case of first-order kinetics the reaction rate is represented as $r = k_1 c_A$, or in terms of sorption efficiency

$$\frac{d\eta}{dt} = k_1(1 - \eta) \quad (1.)$$

where, k_1 is the first order rate coefficient (s^{-1}), c_A stands for the actual concentration of the reactant (mol/L), η the efficiency and t the time (s). The linear form, obtained by integration is

$$-\ln(1 - \eta) = k_1 t \quad (2.)$$

The data were treated based on the supposition that the process can be described by two consecutive first order steps. According to literature [13], the first step represents a rapid complexation on the specific sites of the HAP surface. The second step is attributed either to ion diffusion into the HA structure or to formation of hydroxyapatite containing this heavy metal instead of calcium. Based on this supposition equation (2.) has been plotted with the data for all the non-calcined materials (see figure 3). The slope of the linear part of the curve gives the first order rate constants for the two consecutive steps. The rate constant values and the regression coefficients are presented in table 2. The rate coefficients have higher values for the first step and at lower particle size. The higher calcium concentration of nHAP-Si 5%_{wt} Si as compared to nHAP-Si 5%_{wt} Si does not influence positively the reaction rate. It indicates that the ionic exchange is not the rate determining step. The highest values of the apparent rate constants were calculated for nHAP-Si 10%_{wt} $\Phi < 45 \mu\text{m}$, that is in concordance with the fastest reaction time.

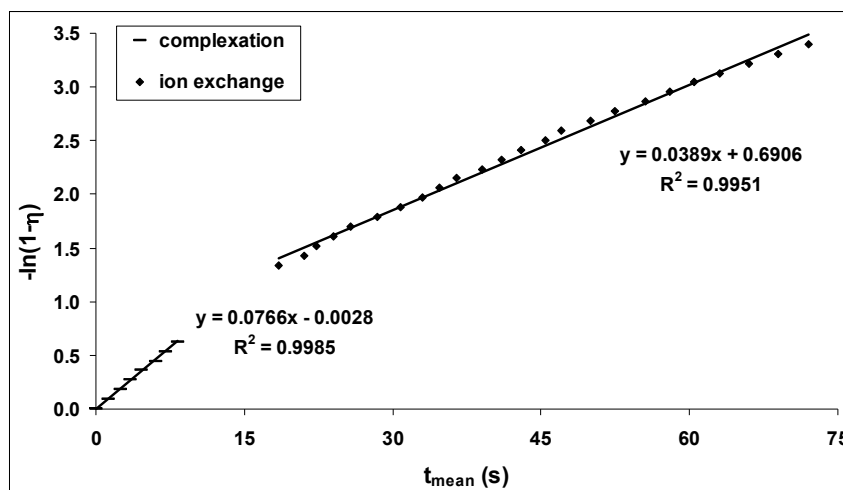


Figure 3. First order kinetics representation for nHAP-Si 10 %wt Si Φ , 45 μm $[\text{Cu}^{2+}] = 1 \text{ mM}$. T=279 K

The pseudo-second order rate model, based on sorbent capacity [14], can be expressed as a differential equation:

$$\frac{dq_t}{dt} = k_2(q_e - q_t)^2 \quad (3.)$$

By integrating this within the same boundary conditions and rearranged, the following linear form is obtained:

$$\frac{1}{q_t} = \frac{1}{k_2 q_e^2} + \frac{1}{q_e} t \quad (4)$$

Here q_t and q_e is amount of solute sorbed on the surface at a time t and at the equilibrium state. A plot of t/q_t versus t should give a straight line with a slope of $1/q_e$ and the intercept of $1/k_2 q_e^2$ (see figure 4). Furthermore, the initial sorption rate h (mmol/g s), when $t \rightarrow 0$, can also be calculated as follows: $h = k_2 q_e^2$ [15,16]. The experimental points lay on the unique straight line over a large period of time. As it can be seen in table 2 the amount of copper ions at equilibrium (mmol/g) is approximately constant for all the materials at the same initial copper (II) concentration. The correlation coefficients for the linear plots for the pseudo-second order rate law are better (>0.995) as compared to the values obtained with the first-order model. This suggests that the system does not obey first-order kinetics, but a pseudo-second order one. According Y. S. Ho and G. McKay [16] in systems described by pseudo-second order model the rate-limiting step may involve some strong interaction (valence forces) between sorbate species and active sites of adsorbent. This model provides the best correlation of the data.

Table 2. Comparison between experimental and calculated amounts of Cu(II) sorbed at equilibrium (q_e), sorption rate constants (k_1 , k_1' and k_2) and corresponding regression coefficients (R^2), for pseudo-first and pseudo-second order kinetic models, at 293 K and $[Cu^{2+}] = 10^{-3}$ M

pseudo-first order								pseudo second order					
$\Phi > 90 \mu m$				$\Phi < 45 \mu m$				$\Phi > 90 \mu m$			$\Phi < 45 \mu m$		
k_1	R^2	k_1'	R^2	k_1	R^2	k_1'	R^2	k_2	q_e	R^2	k_2	q_e	R^2
ncHAP													
0.051	0.997	0.011	0.996	0.118	0.987	0.06	0.995	0.249	0.21	1	1.634	0.206	1
ncHAP-Si 5%_{wt} Si													
0.021	0.996	0.008	0.998	0.097	0.97	0.086	0.994	0.065	0.234	0.999	1.236	0.210	0.999
ncHAP-Si 5%+_{wt} Si													
0.015	0.991	0.008	0.993	0.095	0.978	0.079	0.999	0.069	0.226	0.997	0.819	0.215	0.997
ncHAP-Si 10%_{wt} Si													
0.069	0.99	0.024	0.995	0.071	0.94	0.096	0.985	0.470	0.213	1	1.425	0.218	0.995
ncHAP-Si 15%_{wt} Si													
0.067	0.988	0.007	0.999	0.124	0.991	0.051	0.99	0.219	0.208	1	1.529	0.206	1

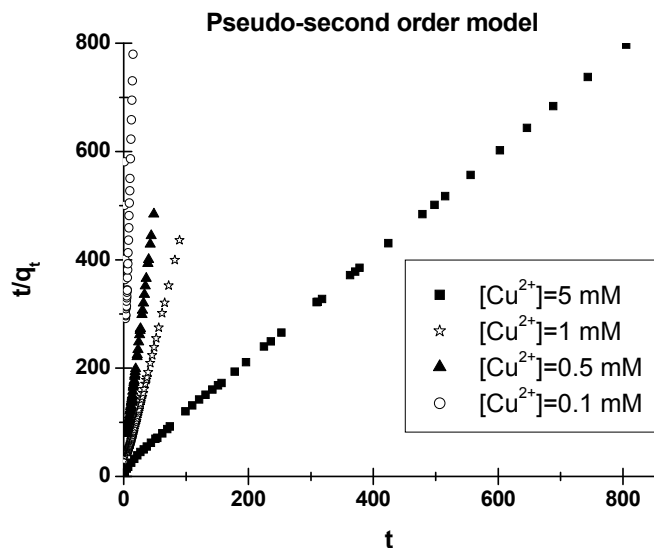


Figure 4. Pseudo-second order rate model for ncHAP-Si 10%_{wt} <45 μm at different initial copper ion concentrations

By using the values of the second order rate constants determined at different temperatures (279, 293, 303, 313, 323 K), the experimental Arrhenius activation energy were obtained for two different concentration and material. The activation energy values are summarized in **Table 3**.

Table 3. Activation energy calculate by Arrhenius type linearization based on pseudo second order rate coefficient values for ncHAP and ncHAP-Si 10%_{wt} Si

Material	[Cu ²⁺] (M)	Φ	10 ⁻³		5 10 ⁻⁴	
			Ea (kJ/mol)	R ²	Ea (kJ/mol)	R ²
ncHAP	>90	>90	35.82	0.972	30.57	0.986
	<45	<45	20.33	0.981	57.46	0.987
ncHAP-Si 10% _{wt} Si	>90	>90	34.73	0.961	42.51	0.993
	<45	<45	42.44	0.985	52.75	0.995

Their values are increased at higher granulometry and concentration, with the exception of ncHAP Φ>90 μm. The activation energies ranges within 20-60 kJ/mol, which indicates that the sorption of copper is not governed only by ion exchange mechanism. Based on literature data, energies between 8–16 kJ/mol are characteristic for the ion-exchange mechanisms [17].

Intraparticle diffusion

The mechanism of sorption is either film diffusion controlled or particle diffusion controlled. Before adsorption takes place, several diffusion processes known to affect the adsorption process takes place. The sorbate, will have to diffuse through the bulk of the solution to the film surrounding the adsorbent and then into the micro pores and macro/ pores of the adsorbent. The first one is bulk diffusion resistance which of course is reduced if there is enough agitation to reduce the concentration gradient. The second is external mass transfer resistance and the third is intraparticle mass transfer resistance. When this last one is the rate limiting step, then sorption mechanism is controlled by intraparticle diffusion.

The model developed by Mackay and Poots [18] can be used to establish the mechanism of sorption.

$$q_t = K_{id} \cdot t^{1/2} + I \quad (5)$$

Where, q_t is the amount of copper ions sorbs at time t . The slope of the linear part of the curve (i.e., q_t Vs $t^{0.5}$) gives the initial rate of the sorption, controlled by intraparticle diffusion K_{id} (mg/g s^{0.5}). The extrapolation of the

straight lines to the time axis gives intercepts I , which are proportional to the boundary layer thickness. The kinetic constants and R^2 values for the intraparticle diffusion model are shown on **Table 4**.

The values of the regression coefficients (R^2) indicate that the model fits the experimental data quite well up to 55-70 % of the process, confirming the intraparticle diffusion in the sorption process. The boundary layer thickness is insignificant. Thus, the boundary layer acts as a viscous drag to the sorption [18].

Table 4. Kinetic constants and regression coefficients (R^2) for Mackay and Poots intraparticle diffusion equation and the efficiency value representative for the linear part of the curve for copper ion sorption on apatites

Material	K_{id}	I	R^2	η (%)
ncHAP $\Phi > 90 \mu\text{m}$	10^{-4}	$3 \cdot 10^{-5}$	0.968	71
ncHAP-Si 5% _{wt} Si $\Phi > 90 \mu\text{m}$	$6 \cdot 10^{-5}$	$4 \cdot 10^{-5}$	0.986	78
ncHAP-Si 10% _{wt} Si $\Phi > 90 \mu\text{m}$	$2 \cdot 10^{-4}$	$2 \cdot 10^{-5}$	0.982	68
ncHAP-Si 15% _{wt} Si $\Phi > 90 \mu\text{m}$	10^{-4}	10^{-4}	0.924	56

CONCLUSIONS

Hydroxyapatite modified with silica was synthesized by addition of sodium silicate to the reaction mixture. These materials were used in copper sorption experiments. The retaining capacity is influenced by calcination, silica content, particle size, initial copper concentration and temperature. Calcined materials show weak metal sorption properties and the silica containing materials have better sorption efficiency than unmodified hydroxyapatite. The 10%_{wt} silica containing hydroxyapatite has the highest copper sorption efficiency. The pseudo-second order model, exhibiting the highest regression coefficients, describes better the sorption of copper onto all the materials. This model agrees with the assumption that the rate-limiting step is chemical sorption or chemisorption involving valence forces between sorbent and sorbate. The activation energies calculated with the pseudo-second order model, in the range of 20-60 kJ/mol also indicate the involvement of chemical interactions. Intraparticle diffusion, irrespective of its mechanism, also plays an important role in this sorption process.

EXPERIMENTAL SECTION

Hydroxyapatite was prepared by the precipitation method described previously [11, 12], under continuous mechanical stirring. The used materials were: 0.5 mol/L solution of calcium nitrate, 0.3 mol/L solution of diammonium phosphate and 25 % ammonia solution (Merck, Germany). The diammonium

phosphate and the ammonium solution were slowly added to the calcium nitrate solution. The reaction mixture pH was adjusted with ammonia to maintain in the range of 9 and 9.5, and the reaction temperature was kept at 20 °C by means of a FALC FA-90 thermostat. The reaction mixture was stirred by FALC mechanical stirrer for 20 hours. For the structurally modified hydroxyapatite, sodium silicate together with the diammonium phosphate and ammonia solution was added to the preparation mixture.

The reaction pH was also adjusted to a value between 9 and 9.5, the temperature was 20 °C and the reaction time was 8 h. Four types of silica-hydroxyapatite (HAP-Si) were prepared: with 5 %, 5 %+, 10 % and 15 mass % of silica. The HAP-Si with 5 %+ of silica content contained by 10 mass % more calcium compared to the other materials. After the reaction was accomplished, the precipitate was washed and filtered. The filtered material was dried for 24 hours at 105 °C. Thermal treatment of the samples was carried out at 1000 °C for one hour, in a Barnstead 47900 furnace.

The characteristics of the materials were established by Infra Red spectroscopy, scanning electron microscopy (SEM), X-ray and BET measurement. The results were presented previously [11, 12].

The prepared materials were employed in kinetic studies of Cu (II) ion retention. Copper nitrate solution was used, in the concentration range between 10^{-4} mol/L and $5 \cdot 10^{-3}$ mol/L. A copper selective electrode (Tacussel PCU 2M) previously calibrated and a reference saturated K^+/KNO_3 electrode were used to monitor copper (II) concentration. A Digitronic DXP-2040 potentiometer was employed. The experiments were carried out in a double walled reactor, connected to a FALC FA-90 thermostat under continuous magnetic stirring, provided by a FALC FA-20 magnetic stirrer. Replicate runs were made and each time, values corresponding to the given potential were averaged.

The reagents were of analytical grade and twice-distilled water was used to prepare all solutions and suspensions. In order to reproduce conditions existing during the purification of waste water, no pH adjustment was made during the experiments. However, pH was monitored with a pH selective electrode during the experiments.

0.25 g sample and 50 mL of copper nitrate solution of different concentrations were used for each experiment. The decrease of electrode potential with time was measured and the data were recorded by a computer. The retained copper quantity, sorption efficiency, and capacity of the material were calculated using the Microsoft Excel and Origin 6.0 software. Analytical detection limit for Cu^{2+} was 5 μ mol/L. The increase calcium ion concentration was registered with a calcium selective electrode. The detection limit was established at $5 \cdot 10^{-7}$ mol/L.

REFERENCES

1. L. A. Landin, L. G. Danielsson, C Wattsgard, *Journal of Bone and Joint Surgery Br*, **1987**, 69-B, 234.
2. J. Zhang, M. Maeda, N. Kotobuki, M. Hirose, H. Ohgushi, D. Jiang, M. Iwasa, *Materials Chemistry and Physics*, **2006**, 99, 398.
3. V. P. Orlovskii, V. S. Komlev, S. M. Barinov, *Inorganic Materials*, **2002**, 38, 10, 973.
4. I. R. Gibson, S. M. Best, W. Bonfield, *Journal of Biomedical Materials Research*, **1999**, 44, 422.
5. M. Vallet-Regí, D. Arcos, *Journal of Materials Chemistry*, **2005**, 15, 1509.
6. F. Balas, J. Pérez-Pariente, M. Vallet-Regí, *Journal of Biomedical Materials Research Part A*, **2003**, 66A, 2, 364.
7. W. Zheng, X.-m. Li, Q. Yang, G.-m. Zeng, X.-x. Shen, Y. Zhang, J.-j. Liu, *Journal of Hazardous Materials*, **2007**, 147, 1-2, 534.
8. F. Fernane, M. O. Mecherri, P. Sharrock, M. Hadioui, H. Lounici, M. Fedoroff, *Materials Characterization*, **2008**, 59, 554.
9. S. McGrellis, J.-N. Serafini, J. JeanJean, J.-L. Pastol, M. Fedoroff, *Separation and Purification Technology*, **2001**, 24, 129.
10. S. K. Lower, P. A. Maurice, S. J. Traina, E. H. Carlson, *American Mineralogist*, **1998**, 83, 147.
11. E. S. Bogya, R. Barabás, A. Csavdári, V. Dejeu, I. Baldea, *Chemical Papers*, **2009**, 63, 5, 568.
12. E. S. Bogya, R. Barabás, L. Bizo, V.R. Dejeu, *Proceedings of the 11th ECERS Conference, Polish Ceramic Society, Krakow*, **2009**, 1109-1113, ISBN: 978-83-60958-54-4.
13. A. Corami, S. Mignardi, V. Ferrini, *Journal of Hazardous Materials*, **2007**, 146, 1-2, 164.
14. I. Smiciklas, A. Onjia, S. Raicević, D. Janačković, M. Mitrić, *Journal of Hazardous Materials*, **2008**, 152, 876.
15. M. Fedoroff, G. Lefevre, M. Duc, S. Milonjic, C. Neskovic, *Materials Science Forum*, **2004**, 453-454, 305.
16. Y.S. Ho, G. McKay, *Process Biochemistry*, **1999**, 34, 451.
17. S. S. Dimovic, I. Plecas, M. Mitric, *Water Research*, **2006**, 40, 2267.
18. J. C. Igwe, O. F. Mbonu, A. A. Abia, *Journal of Applied Science*, **2007**, 19, 2840.